

Analytical model of the transversal flux inductor

Monica Popa* and Virgiliu Firețeanu**

*University of Oradea, Faculty of Electrical Engineering and Information Technology
str. Universitatii nr. 1, 410087 Oradea, Romania, mpopa@uoradea.ro

** POLITEHNICA University of Bucharest, EPM_NM Laboratory

Abstract – This paper deals with the computation based on an analytical model of the induced currents, the density of the active power in the sheet to be heated, the transversal profile of this density integrated along the sheet and the efficiency of an induction heating system for thin sheets of transversal flux type. The analytical model uses a database that contains set of results of 3D numerical modeling performed with Flux3D. The analytical model is a useful tool for fast computation and can be easily coupled with an optimization procedure in order to obtain a minimum non-uniformity of the transversal profile of induced power in the sheet.

Keywords: induction heating, transversal flux, analytical model

I. INTRODUCTION

The main steps for the analytical computation of the transverse flux inductor as follows:

- evaluation of longitudinal and transversal variation of electromagnetic field source;
- computation of the two components $J_{2x}(x,y)$ and $J_{2y}(x,y)$ of the induced current density on the metallic sheet by Fourier series with respect the coordinate x and by finite differences with respect the transversal coordinate y ;
- evaluation of volume power density induced in the metallic sheet (constant on thickness);
- evaluation of transversal profile $Profil(y)$ of the induced power density integrated along the inductor;
- computation of the deviation of transversal profile;
- evaluation of the power losses in the inductor coils, cooper screens, magnetic cores lateral clamping plates included and the computation of inductor electrical efficiency

II. LONGITUDINAL AND TRANSVERSAL VARIATION OF THE ELECTROMAGNETIC FIELD SOURCE

The source of electromagnetic field is an equivalent current density of amplitude J_{1m} . This density is the result of the assumption that the real source, which is the

total current in the coils, is uniformly distributed in air-gap. The longitudinal variation of this current density along the air-gap, Fig. 1, expressed by harmonic functions, Fig. 2, has for $x \geq 0$ the following form:

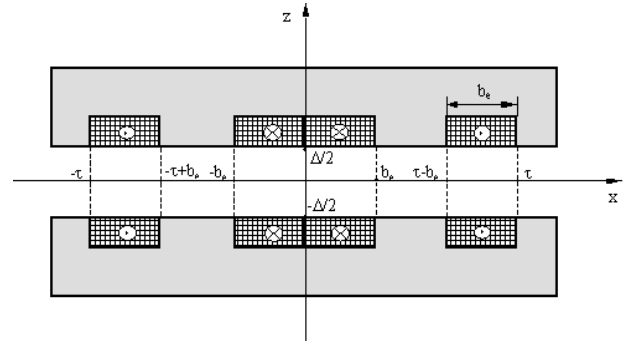


Fig. 1. Inductor longitudinal section

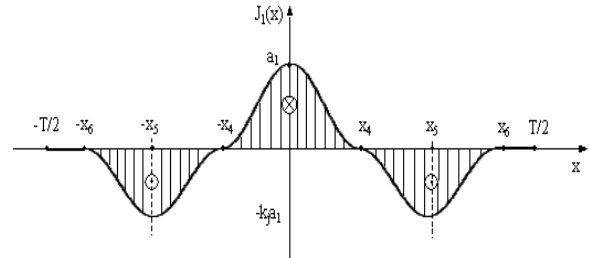


Fig. 2. Longitudinal variation of the electromagnetic field source

$$J_1(x) = \begin{cases} \frac{a_1}{2} \left(1 + \cos \frac{\pi x}{x_4}\right), & x \in [0, x_4] \\ -\frac{k_j a_1}{2} \left[1 + \cos \frac{\pi(x - x_5)}{x_5 - x_4}\right], & x \in (x_4, x_5] \\ -\frac{k_j a_1}{2} \left[1 + \cos \frac{\pi(x - x_5)}{x_6 - x_5}\right], & x \in (x_5, x_6] \\ 0, & x \in (x_6, T/2] \end{cases} \quad (1)$$

The current density amplitude J_{1m} of the equivalent source as a function of total current (NI_1) in a coil is given by the relation:

$$J_{1m} = \frac{\sqrt{2}(NI_1)}{b_e(\Delta/2)} \quad (2)$$

Expressed by Fourier series the transversal model (1) is:

$$J_1(x) = \sum_{k=1,2,3} J_{1k} \cos \frac{2k\pi x}{T}, \quad (3)$$

The amplitude of the harmonics k J_{1k} has the expression:

$$J_{1k} = \frac{a_1}{k\pi} (1+k_j) \sin \frac{2k\pi x_4}{T} - \frac{k_j a_1}{k\pi} \sin \frac{2k\pi x_6}{T} + \frac{a_1}{T} \left(\frac{\sin p_1 x_4}{p_1} + \frac{\sin p_2 x_4}{p_2} \right) - \frac{k_j a_1}{T} \left[\frac{\sin(p_3 x_5 - q_3) - \sin(p_3 x_4 - q_3)}{p_3} + \frac{\sin(p_4 x_5 - q_3) - \sin(p_4 x_4 - q_3)}{p_4} \right] - \frac{k_j a_1}{T} \left[\frac{\sin(p_5 x_6 - q_5) - \sin(p_5 x_5 - q_5)}{p_5} + \frac{\sin(p_6 x_6 - q_5) - \sin(p_6 x_5 - q_5)}{p_6} \right] \quad (4)$$

where $p_1 = \frac{\pi}{x_4} + \frac{2k\pi}{T}$, $p_2 = \frac{\pi}{x_4} - \frac{2k\pi}{T}$, $p_3 = \frac{\pi}{x_5 - x_4} + \frac{2k\pi}{T}$,
 $p_4 = \frac{\pi}{x_5 - x_4} - \frac{2k\pi}{T}$, $p_5 = \frac{\pi}{x_6 - x_5} + \frac{2k\pi}{T}$, $p_6 = \frac{\pi}{x_6 - x_5} - \frac{2k\pi}{T}$
 $q_3 = -\frac{\pi x_5}{x_5 - x_4}$, $q_5 = -\frac{\pi x_5}{x_6 - x_5}$ (5)

A number of terms in Fourier series greater than 10 ensures a very good source representation.

Evaluation of longitudinal variation of electromagnetic field source, respectively the computation of the quantities x_4 , x_5 , x_6 and k_j in (1) is performed by the interpolation of the results of Flux3D gathered in a data file [1].

In order to take into account the variation of magnetic field along a direction normal to the sheet in the real inductor the quantity J_{1m} is multiplied by a correction factor k_z .

Fig. 3 presents half of the cross section $y > 0$ through the studied transversal flux inductor with one pair of fix magnetic cores and two pairs of mobiles magnetic cores. The metallic sheet of thickness A and width $B/2$ is placed in the inductor symmetry plane $z = 0$.

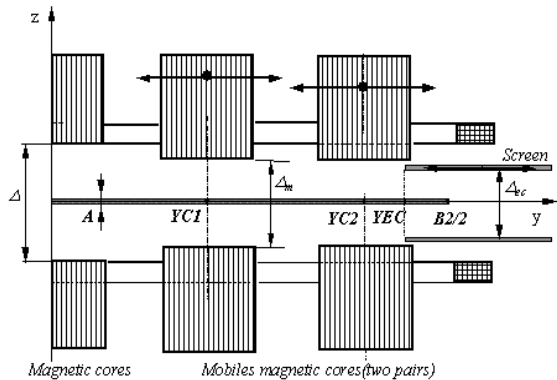


Fig. 3. Cross section through the transversal flux inductor

For every set of input data (YC1, YC2, YEC) which express the position of mobile cores and screen the function that express the relative transversal variation of source $VAR_TRANSV_SOURCE(y)$ is achieved by the

interpolation of the results of Flux3D gathered in a data base [1].

III. COMPUTATION OF INDUCED CURRENTS DENSITY AND OF INDUCED POWER DENSITY

The analytical computation of induced currents density is based on the following assumptions:

- an inductor equivalent with the real one, having ideal magnetic cores, Fig. 4, with infinite width and length;

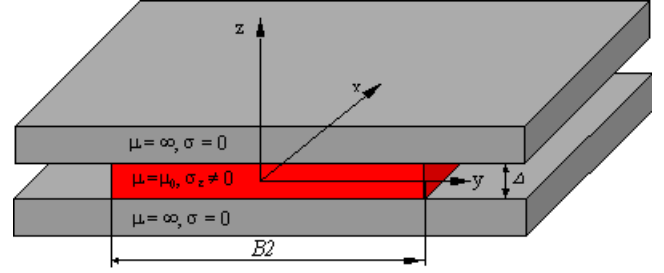


Fig. 4. The equivalent transversal flux inductor

- the real source of electromagnetic field is replaced by an equivalent current density $\underline{J}_1[0, J_1(x,y), 0]$, with orientation along the coordinate y , Fig. 4, in whole air-gap of thickness Δ . The amplitude of the equivalent current density is given by equation (2).
- the real metallic sheet of width $B/2$, thickness A and electrical conductivity $\sigma = 1/RO$ is replaced by an equivalent one of the same width, nonmagnetic, thickness Δ and conductivity σ_e . The equivalent quantity σ_e satisfies the equality $\sigma_e \cdot \Delta = \sigma \cdot A$

As a consequence of the above assumptions the electromagnetic field within the air-gap of equivalent inductor does not vary along Oz axis, Fig. 4 and the induced currents density \underline{J}_2 has two components, along axes Ox et Oy , $\underline{J}_2[J_{2x}(x,y), J_{2y}(x,y), 0]$.

The complex form of Maxwell equations in the region sheet equivalent is:

$$\begin{aligned} \text{rot } \underline{E} &= -j\omega \underline{B} \\ \text{rot } \underline{H} &= \underline{J}_1 + \underline{J}_2 \\ \underline{J}_2 &= \sigma_e \underline{E} \\ \underline{B} &= \mu_0 \underline{H} \end{aligned} \quad (6)$$

The unknown component $J_{2y}(x, y)$ of induced currents satisfies the following equation:

$$\left(\frac{\partial^2}{\partial x^2} + \frac{\partial^2}{\partial y^2} \right) J_{2y}(x, y) = j\omega \mu_0 \sigma_e [J_1(x, y) + J_{2y}(x, y)] \quad (7)$$

The evaluation of J_{2y} takes into account the following boundary conditions:

$$\underline{J}_{2y}(x, b) = 0 \text{ and } d\underline{J}_{2y}(x, y)/dy|_{y=0} = 0 \quad (8)$$

According to the equation (3) $J_1(x,y)$ is expressed by the formula:

$$J_1(x,y) = \sum_k J_{1k}(y) \cos \alpha_k x, \alpha_k = 2k\pi/T \quad (9)$$

Equation (7) imposes that the component $J_{2y}(x,y)$ of induced currents density has the same variation as the source density in relation with variable x :

$$J_{2y}(x,y) = \sum_k J_{2yk}(y) \cos \alpha_k x \quad (10)$$

The condition of zero divergence of induced current densities in region sheet imposes the following form of the component $J_{2x}(x,y)$ of the current density:

$$J_{2x}(x,y) = \sum_k J_{2xk}(y) \sin \alpha_k x \quad (11)$$

The amplitude $J_{2xk}(y)$ in (11) satisfies the equation:

$$J_{2xk}(y) = - \left[\frac{dJ_{2yk}(y)}{dy} \right] / \alpha_k \quad (12)$$

The amplitudes $J_{2yk}(y)$ in eq. (10) and (12) are the solutions of differential equations:

$$\frac{d^2 J_{2yk}(y)}{dy^2} - \lambda_{1k}^2 J_{2yk}(y) = \lambda_{1k}^2 J_{1k}(y) \quad (13)$$

where $\lambda_{1k}^2 = j\omega\mu_0\sigma_e + \alpha_k^2$ and the boundaries conditions:

$$J_{2yk}(B/2) = 0 \quad \text{and} \quad \left. \frac{dJ_{2yk}}{dy} \right|_{y=0} = 0 \quad (14)$$

The equivalent current source density has the expression:

$$J_1(x,y) = \sum_{k=1,2,3,\dots} J_{1k}(y) \cos \frac{2k\pi x}{T}, \quad \text{with } T = 3\tau, \quad (15)$$

where $J_{1k}(y) = J_{1k}(k) \cdot VAR_TRANS_SOURCE(y)$ and $J_{1k}(k)$ has the expression (4).

A numerical finite difference solution is applied to the mathematical model represented by equations (13), (14) and (12).

Following the evaluation of the components $J_{2x}(x,y)$ and $J_{2y}(x,y)$ of induced currents density in the domain $x \in [-T/2, T/2]$, $y \in [0, B/2]$, the induced volume power density in sheet equivalent is computed by the relation:

$$p_{J2}(x,y) = \frac{1}{2\sigma_e} |J|^2 = \frac{1}{\sigma_e} [|J_{2x}(x,y)|^2 + |J_{2y}(x,y)|^2] \quad (16)$$

The surface density of induced power in real sheet is evaluated through the equation:

$$p_{J2s}(x,y) = p_{J2}(x,y)\Delta \quad (17)$$

The transversal profile of the induced power density integrated along the sheet is expressed by the formula:

$$Profil(y) [\%] = 100 \frac{p_{J2i}(y) - p_{J2i}(0)}{p_{J2i}(0)} \quad (18)$$

where:

$$p_{J2i}(y) = \int_0^{T/2} p_{J2}(x,y) dx, \quad p_{J2i}(0) = \int_0^{T/2} p_{J2}(x,0) dx \quad (19)$$

The induced power in sheet, P_2 , is the result of computing the following integral:

$$P_2 = \frac{4\Delta}{\sigma_e} \int_0^{T/2} \int_0^{B/2} p_{J2}(x,y) dx dy \quad (20)$$

IV. NUMERICAL APPLICATIONS OF ANALYTICAL MODEL

The dedicated tool developed on the base of analytical model yields the following graphical and numerical results:

- the transversal variation of electromagnetic field source;
- the 3D image of the longitudinal and transversal variation of electromagnetic field source ;
- the 3D image of the induced surface power density $p_{J2s}(x,y)$;
- the chart of the power density $p_{J2s}(x,y)$;
- the transversal profile of induced power density, *Profil(y)* ;
- the deviation of transversal profil, *Ecart_Profil*.
- the induced power P_2 in the sheet ;
- the power losses in coils, in screens, in lateral clamping plates and the magnetic core losses ;
- the inductor electrical efficiency.

Results are presented below.

A graphical user interface was created.

Donnees tole	Alimentation	Positions actionneurs
Largeur tole, B2 [mm] 858 <- B2 <- 1558 1200	Frequence, f [Hz] 500 <- f <- 2000 1500	Position culasse C1, YC1 [mm] 225.5 <- YC1 <- 493.5 350
Epaisseur tole, A [mm] 0.29 <- A <- 2.5 0.5	Amperspires des encoches extremes [A] 1400	Position culasse C2, YC2 [mm] 493 <- YC2 <- 642.5 500
Resistivite, RO [Ohm mm ² /m] 0.2 <- RO <- 1.2 1.2		Position ecran, YEC [mm] 397 <- YEC <- 643 400

CONTINUER >>

Fig. 5. Window for data input

The input data of an analytical computation are: B2, A, RO, f, NI₁, YC1, YC2, YEC.

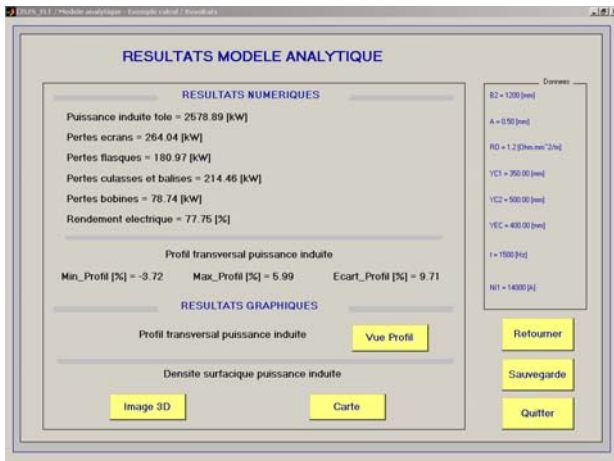


Fig. 6. Numerical results window

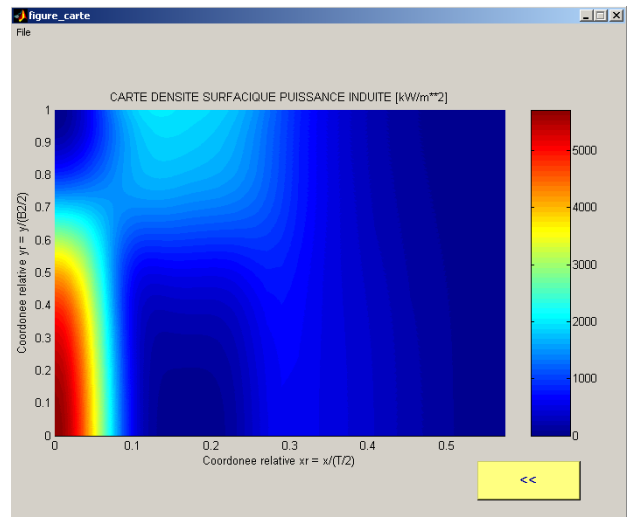


Fig. 9 Chart of the induced surface power density

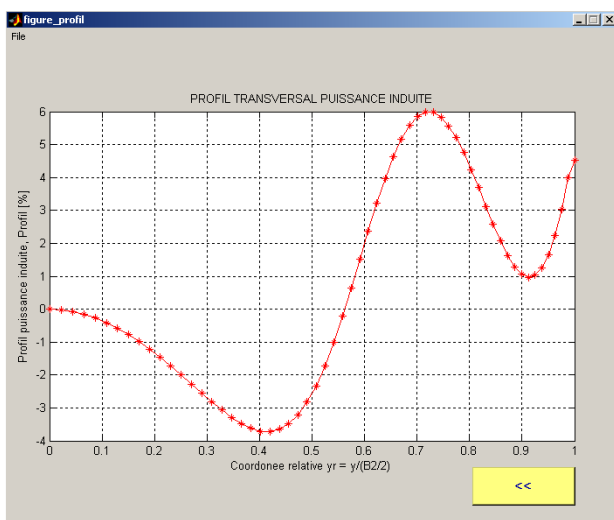


Fig. 7 - Transversal profile of induced power density, rel. (18)

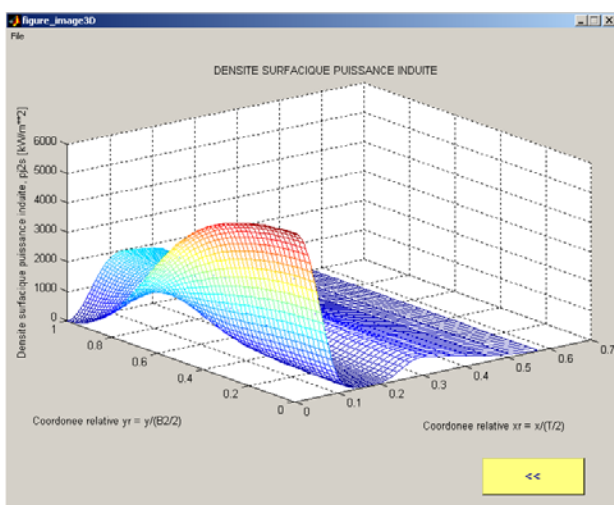


Fig. 8 - Induced surface power density, rel. (17)

V. CONCLUSIONS

The analytical model presented in this paper, based on input data issued from finite element 3D analysis, was implemented in an efficient tool for very fast computation and optimization of transversal flux inductors with flexible electromagnetic configuration, including mobile magnetic cores and eddy current screens.

Preliminary optimal positions of the mobile components of the inductor with respect the minimum transversal non-uniformity of the temperature can be easily defined, before refining the investigation for the best design solution with finite element analysis.

REFERENCES

- [1] V. Fireteanu, M. Popa, T. Tudorache - Simulation numeriques en flux transverse – Rapport contrat recherche, no JYR/VR/L2579, 2004
- [2] H. Schulse, A. Nikanorov, B. Nacke – Flexible transverse flux heaters of metal strip – Proc. of HES-04 Symposium, Padua, 2004
- [3] F. Dughiero, S. Lupi, A. Muhlbauer, A. Nikanorov – TFH – transverse flux induction heating of non-ferrous and precious metal strips. Results of a EU research project, *COMPEL Revue*, Vol. 22, 2003